OBSERVATIONS ON COTR DUE TO THE MICROBUNCHING INSTABILITY IN COMPRESSED BEAMS*

A.H. Lumpkin, Fermilab, Batavia, IL U.S.A. 60510
Y. Li, S.J. Pasky, and N.S. Sereno
Argonne National Laboratory, Argonne, IL U.S.A. 60439

Abstract

The observations of the strong enhancements of the optical transition radiation (OTR) signal observed after bunch compression of photocathode beams in the Advanced Photon Source (APS) linac chicane continue to be of interest. These effects have been attributed to a microbunching instability. Recent tests with an Oriel spectrometer with ICCD readout have extended our COTR spectral studies. In this case we used a microchannel plate image intensifier with a GaAs photocathode to explore the NIR regime out to 880 nm. We report for the first time an ~40% intensity modulation of ~25-nm period throughout the observed broadband COTR spectra for some localized spatial structures. In addition, the observation of a ring-like COTR image structure in x-y space for a mismatched beam at 355 MeV and a COTR mitigation concept will be presented and discussed.

INTRODUCTION

An improved understanding of the strong enhancements of the optical transition radiation (OTR) from bright linac beams following bunch compression is occurring as evidenced by recent reports in workshops and conferences in the last few years [1-5]. The observed features are attributed to a combination of longitudinal space charge (LSC) effects in a linac, coherent synchrotron radiation (CSR) effects, and a Chicane compression process [4]. There appears to be a microbunching instability such that broadband coherent OTR (COTR) is generated in the visible wavelength regime. Such enhancements prevent the normal beam-profiling measurements with OTR monitors at the Linac Coherent Light Source (LCLS) and the Advanced Photon source (APS). Since the APS injector complex includes a chicane bunch compressor and we have microbunching interests [6], we decided to study these COTR effects more extensively.

Spectral-dependence measurements of the COTR were done initially at the 375-MeV station with bandpass filters and a CCD camera readout of the imaging spectrometer [7], but the recent tests with an ICCD camera readout have extended those studies to the NIR and confirmed newly proposed mitigation concepts. These latter techniques are complementary to the proposed use of a laser heater to mitigate the microbunching at LCLS [8].

*Work supported by U.S. Department of Energy, Office of Science, Office of High Energy Physics, under Contract No. DE-AC02-06CH11357.

EXPERIMENTAL BACKGROUND

The measurements were performed at the APS facility which includes an injector complex with two rf thermionic cathode (TC) guns for injecting an S-band linac that typically accelerates the beam to 325 MeV, the particle accumulator ring, the booster synchrotron that ramps the energy from 0.325 to 7 GeV in 220 ms, a booster-to-storage-ring transport line, and the 7-GeV storage ring. In addition, there is an rf photocathode (PC) gun that can also be used to inject into the linac as shown schematically in Fig. 1 of reference [3]. An extensive diagnostics suite is available in the chicane and after the chicane area. The tests were performed in the linac at the three imaging stations after the chicane bunch compressor and at the end of the linac where another beam imaging station is located. A FIR coherent transition radiation (CTR) detector (Golay cell) and Michelson interferometer [3] are located between the second and third screen of the three-screen emittance stations. A vertical bend dipole and diagnostics screens in this short beamline allow the monitoring of tranverse x beam size and energy following compression The YAG:Ce emission and OTR were directed by turning mirrors and relay optics to a Pulnix CCD camera located 0.5 m from the source. These Chicane stations also have options for low- and high-resolution imaging of the beam spot by selecting one of two lens configurations [9].

At the end of the linac, the imaging station (Sta-5) included the optical transport of the visible light out of the tunnel to a small, accessible optics lab where the CCD camera was located. This allowed the access for exploring the spectral dependency of the enhanced OTR. A set of bandpass filters with center wavelengths in 50-nm increments from 400 to 750 nm and 40-nm band width as well as a 500-nm shortpass filter and 500-nm long pass filter were used in the initial tests [7]. Recently the spectral measurements were extended by adding an optional transport path to an Oriel UV-visible spectrometer with two readout ports. One port used a Vicon 2400 CCD, and the other used an ICCD as shown in Fig. 1. For these experiments we installed a GaAs photocathode microchannel-plate-intensified CCD camera, Pulnix model DN007. This device has a strong, flat response or quantum efficiency (Q.E.) from 550 to 880 nm in the NIR as shown in Fig. 2 [10]. The GaAs Q.E. does roll off rapidly at each end of this range. The OTR and YAG:Ce images were recorded with a Datacube MV200 video digitizer for both online and offline image analyses, and a video switcher was used to select the

camera signal for digitizing. The beam energy was 375 MeV at the location of this imaging station.

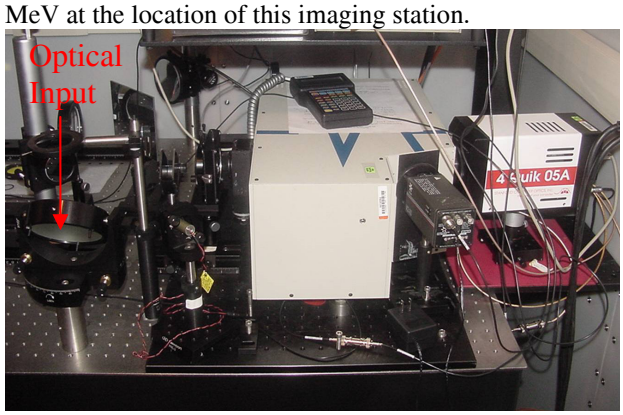

Figure 1: Photograph of the transport optics, Oriel Spectrometer, and two readout cameras for Sta-5.

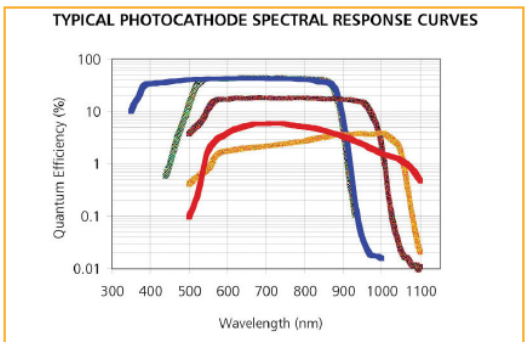

Figure 2: The microchannel plate's GaAs photocathode spectral response or Q.E. in the visible and near IR. The green curve which overlaps with the blue curve from 550 nm to 880 nm is the relevant one [10].

BUNCH COMPRESSION

We have previously reported a series of experiments on the LSCIM [11, 12]. Those experiments were initiated by transporting the PC gun beam accelerated to 150 MeV to the chicane area. The rf phase of the L2 accelerator structure located before the chicane was used to establish the appropriate conditions for compression in the chicane. The degree of compression was tracked with the Golay cell signals. A very strong variation of the FIR CTR signal correlated with L2 phase was observed. There was almost no signal seen when uncompressed and 300 units seen at the peak compression. The autocorrelation scan was then performed and showed a profile width of ~65 µm (FWHM) as shown in Fig. 10 of reference [3]. This would mean a path length difference between the mirrors of 130 µm, or about 430 fs (FWHM). The initial PC gun drive laser bunch length was 3 to 4 ps (FWHM). The PC gun beam bunch length depends on rf gun phasing and charge density.

The reconstruction of the time profile was performed by the standard practices as described previously [13]. A bunch length of less than 400 fs [FWHM] with a leading-edge spike was indicated for the PC gun beam. Subsequently the TC gun beam was also compressed and a similar autocorrelation was performed [7]. The zero phasing rf technique was also used to evaluate the compressed bunch length of the PC gun beam and a result of 550 fs rms was obtained. The leading edge spike however has a FWHM of ~440 fs as seen in Fig. 1 of reference [7].

COTR SPECTRAL RESULTS WITH PC RF GUN BEAMS

In order to assess the spectral dependency of the OTR enhancements, we accelerated the beam to 375 MeV and imaged the beam spot with OTR at a downstream station. As described previously, this station included transport of the signal outside of the tunnel to a small optics lab. We routinely see enhanced localized spikes when we have compressed the beam sufficiently. While adjusting the compression, we made our first observations of a spectral intensity modulation throughout the span of the GaAs PC as shown in Fig. 3. The full span is 300 nm from 600 to 900 nm, but the PC's Q.E. drops at about 880 nm.The pseudo color intensity mapping in the image shows the somewhat regularly spaced intensity peaks in yellow. The spectral profile at the right was taken through the stronger localized x position at line 200. The intensity modulation peak to valley is about 40% in some regimes, but this may be a ±20% modulation around an intensity envelope. The peak spacing is about 17 nm to 31 nm for central wavelengths of 600 nm to 800 nm, respectively, determined by graphical analyses.

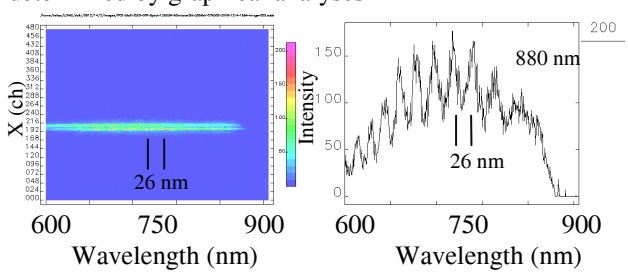

Figure 3: Imaging spectrometer spectrum of the NIR COTR near maximum compression conditions. The image (L) and profile (R) through the enhanced x location at line 200 are shown. This grating had 95 lines per mm.

As part of the assessment of the source of the effect we changed gratings in the spectrometer to 135 lines/mm as seen in Fig. 4. In this case after locating the similar wavelengths to Fig. 3, we see different spacings of the peaks in pixels, but similar in wavelength after applying the calibration factor. Still these spacings are a little larger for this case, and with this less intense effect the envelope also appears flatter across the span of coverage. We also showed the modulation persisted with an offset or grating angle change in the spectrometer. We note that we have not seen such an effect with TC rf gun beam tests to date.

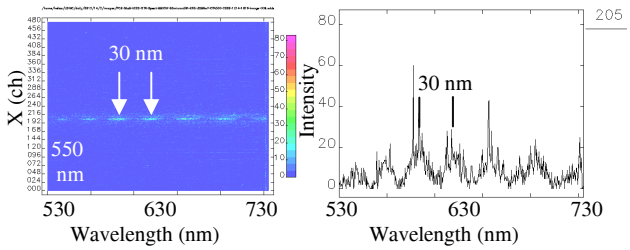

Figure 4: Imaging spectrometer spectrum of the NIR COTR near maximum compression conditions. The image (L) and profile (R) through the enhanced x location are shown. This grating had 135 lines per mm.

The spectral modulation may result from multiple temporal pulses, with the temporal modulation manifesting itself in the spectral modulation via Fourier transformation. In this case $d\nu = 1/dt$ where $d\nu$ and dt are the modulation period in the frequency and time domain, respectively. From the spectra, we have $d\nu = -c\, d\lambda/\lambda^2 = 14.1 \times 10^{12}$ s^{-1} for λ=600 nm and a spacing of $d\lambda$=17 nm and $d\nu$=13.3 x 10^{12} s^{-1} for λ=750 nm and $d\lambda$= 25 nm. These two frequencies correspond to a z period of 21 and 22 µm, or a dt of about 70 and 73 fs, respectively. The case in Fig. 4 seems to be ~40% shorter in period. The results are summarized in Table I for the two cases. Interestingly, such modulation periods are in the region of expected strong gain for the LSC microbunching instability as reported previously [8]. We can exclude double-pulse emission from the cathode as the origin because the modulation period does not correspond to any characteristic time in the laser system after accounting for the compression factor.

Table I: Summary of observations on the COTR spectral modulation with the two gratings in the Fig. 3 and Fig. 4 cases. The grating, wavelength, peak separation (Sep.), modulation frequency (Mod. Freq.), and modulation period are given.

Grating Lines/mm	Wavelength (nm)	Peak Sep. (nm)	Mod. Freq. (THz)	Mod. Period (µm)
95	600	17	14.1	21
95	650	19	13.5	22
95	700	23	14.1	21
95	750	26	13.9	22
95	800	31	14.5	21
135	550	25	24.8	12
135	600	30	25.0	12
135	650	31	22.0	14
135	700	36	21.8	14

RING-LIKE STRUCTURE

In the course of our investigations we transported compressed beam to the Sta-5 at the end of the linac. Our initial observation with the CCD camera focused at the screen surface was the image at the left. A ring-like pattern of COTR enhancements was observed at the perimeter of the large, defocused image. These were under mismatched conditions for the upstream quadrupoles located at the end of the linac. We could make the ring collapse in diameter to the smaller spot at the right by either changing the accelerator phase (beam energy) or adjusting the quadrupole strengths. In both latter cases the ring-like structures were no longer seen.

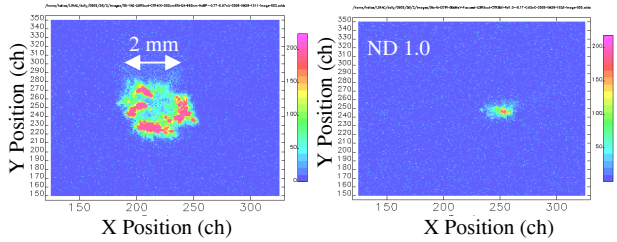

Figure 5: Images of COTR at 355 MeV under mismatched (L) and matched (R) lattice conditions. ND 1.0 was added to the focused image.

MITIGATION OF COTR EFFECTS

For completeness for the FEL09 conference , we discuss the mitigation of COTR effects in the beam profiling screens based on a combination of experimental techniques described elsewhere [12]. The principal issue is to improve the OTR signal to COTR ratio by imaging in the violet to UV end of the spectrum. This is graphically illustrated in Fig. 6 where the relative OTR intensity dependence on $1/\lambda^2$ is shown. We compare this to an example of the OTR multiplied by the COTR gain factor for a 3-keV slice energy spread term as calculated in reference [14]. It is clear that for this scenario a bandpass filter centered at 400 nm would suppress or mitigate the COTR contributions.

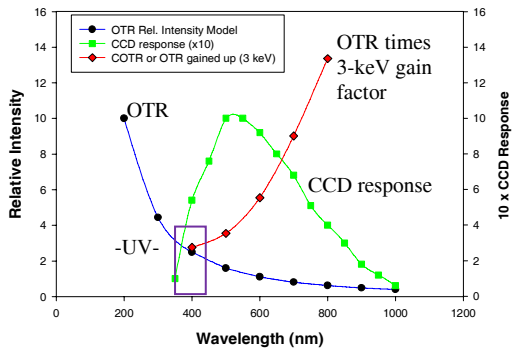

Figure 6: Analytical representations of the OTR dependence on $1/\lambda^2$ and OTR times the 3-keV gain factor, or COTR. The CCD camera response is also shown.

We can also combine the suppression of the COTR with the 400-nm BPF and the response of the LSO:Ce crystal to produce a beam profile image that is not corrupted by COTR spikes as shown in Fig. 7 (right). Additionally, one could use solar blind or UV filters with UV sensing cameras to select 380 to 200 nm OTR with reduced COTR.

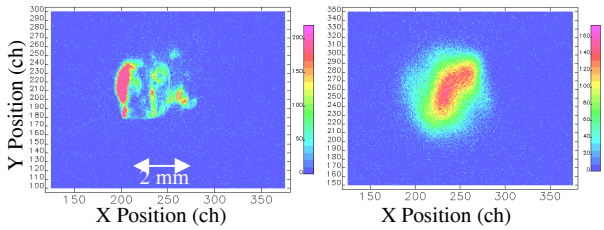

Figure 7: Beam Images via COTR from an Al mirror (L) and the 400-nm bandpass filtered LSO:Ce crystal emissions plus any Al mirror COTR (R).

SUMMARY

In summary, we have characterized the COTR spectral content and extended our studies into the NIR. We observed for the first time a strong spectral intensity modulation that seems to be related to THz microbunching. We also reported a ring-like structure under mismatched beam conditions. We then reported the mitigation of the COTR spikes by using a violet bandpass filter with the option of an LSO:Ce crystal. Further investigations are needed as well as a more complete characterization of the drive laser and linac beam properties for input to simulations.

ACKNOWLEDGEMENTS

The authors acknowledge support from R. Gerig, K.-J. Kim, and H. Weerts of the Argonne Accelerator Institute and M. Wendt of Fermilab. They also acknowledge the controls support by S. Shoaf of ANL for the relocated spectrometer and cameras and discussions with B. Yang of APS and Z. Huang of SLAC. We wish to thank Dr. A. Ting and the Naval Research Laboratory for the use of their photocathode rf gun.

REFERENCES

[1] D.H. Dowell et al., "LCLS Injector Commissioning Results", Proc. of FEL07, Aug. 26-30, 2007, Novosibirsk, Russia.

[2] Agenda for Workshop on "Microbunching Instabilities", Berkeley, October 6-8, 2008.

[3] A.H.Lumpkin et al., "Observations of Enhanced OTR Signals from a Compressed Electron Beam", submitted to proceedings of BIW08, May 4-8, 2008.

[4] Z. Huang et al., "COTR and CSR from Microbunched LCLS Beam", Proc. of CHBB, Zeuthen, May 26-30, 2008.

[5] A.H. Lumpkin et al., Proc. of FEL05, JACoW/eConf C0508213, 608 (2005).

[6] A.H. Lumpkin et al., Phys. Rev. Lett., Vol. 86(1), 79, January 1, 2001.

[7] A.H. Lumpkin et al., "Spectral and Charge-Dependence Aspects of EOTR ", TUP087, Proc. of Linac08, Victoria, Canada, Sept.28-Oct.2,2008.

[8] Z. Huang et al., Phys. Rev.ST Accel. Beams **7**, 074401(2004).

[9] B.Yang et al., BIW2002, AIP Conf. Proc. 648, 393 (2002).

[10] For example, see the ITT data sheets for the Pulnix DN007 intensified CCD camera.

[11] A.H. Lumpkin, R.J. Dejus, and N.S. Sereno, Phys. Rev. ST-AB **12,** 040704 (2009).

[12] A.H. Lumpkin, N.S. Sereno,W.J. Berg, M. Borland, Y. Li, and S.J. Pasky, Phys. Rev. ST-AB August 2009.

[13] N.S. Sereno, M. Borland, A.H. Lumpkin, MOB17, Proc. of Linac 2000, Monterey Ca.

[14] D.Ratner, A. Chao,and Z. Huang, Proc.of FEL08, Gyeongju, Korea, TUPPH041, August 24-29, 2008.